Cyclic operation of a fixed-bed pressure and temperature swing process for CO_2 capture: Experimental and statistical analysis

S. García, M.V. Gil, J.J. Pis, F. Rubiera, C.Pevida[1]

Instituto Nacional del Carbón, INCAR-CSIC, Apartado 73, 33080 Oviedo, Spain

Abstract

An adsorption process that effectively separates CO_2 from high pressure CO_2/H_2 shift gas streams to meet the requirements of pre-combustion CO_2 capture has been evaluated. A commercial activated carbon, Norit R2030CO2, was used as the adsorbent material and different batchwise regeneration conditions were investigated. Statistical analysis by means of Response Surface Methodology (RSM) was employed to assess the combined effect of three independent variables, namely, desorption temperature (T_{des}), desorption pressure (P_{des}) and purge to feed ratio (P/F ratio) on the adsorbent performance. A bench-scale fixed-bed reactor enabled the simulation of the adsorption, heating and depressurization steps of a pressure and temperature swing adsorption-based process. Experimental data were then assessed by the statistical technique and a set of mathematical equations that describes the behaviour of the given set of data was generated. No interaction effects between the independent variables on the responses were found. P/F ratio was found to be the most influential variable on working adsorption capacity, CO_2 recovery, adsorbent productivity and H_2 and CO_2 purities. The maximum CO_2 purity was obtained at 60 ºC, 5 bar and a P/F ratio of 0.05. On the other hand, desorption temperature had the largest impact on the maximum rate of desorption.

Keywords: Response surface methodology; cyclic dynamic experiments; pressure and temperature swing adsorption; CO_2/H_2 separation; sorbent performance; activated carbon.

Notation

T_{des}	desorption temperature, [ºC]
P_{des}	desorption pressure, [bar]
P/F ratio	purge to feed ratio

[1]Corresponding author. Tel.: +34 985 11 89 87; fax: +34 985 29 76 62.
E-mail address: cpevida@incar.csic.es

q_{CO2}	CO_2 working capacity, [mol CO_2/kg adsorbent]
$r_{max\ des}$	maximum rate of desorption, [%v/v min^{-1}]
y	response variable
x_1, x_2, x_3	independent variables
β_0	constant term
$\beta_1, \beta_2, \beta_3$	coefficients of the linear parameters
$\beta_{11}, \beta_{22}, \beta_{33}$	coefficients of the quadratic parameters
$\beta_{12}, \beta_{13}, \beta_{23}, \beta_{123}$	coefficients of the interaction parameters
ε	residual value
R^2	coefficient of determination
Adj-R^2	coefficient of determination adjusted by the number of variables

Acronyms

CCS	Carbon Capture an Storage
IGCC	Integrated Gasification Combined Cycle
PSA	Pressure Swing Adsorption
TSA	Temperature Swing Adsorption
PTSA	Pressure and Temperature Swing Adsorption
AC	Activated carbons
RSM	Response Surface Methodology
STP	standard temperature and pressure
TCD	thermal conductivity detector
ANOVA	analysis of variance
DF	degrees of freedom

1. Introduction

Carbon capture and storage (CCS) is widely acknowledged as a way of seriously contributing to the reduction of CO_2 emissions from large-point stationary sources. Integrated gasification combined cycle (IGCC) is a technology that uses the syngas generated from the gasification of different hydrocarbons, mainly heavy petroleum residues, to fuel a combined cycle power plant. Should this technology be used in conjunction with CO_2 capture, i.e., pre-combustion capture, the CO in the syngas has to

be converted to CO_2 and H_2 by a shift reaction. CO_2 would be then separated from the H_2 to be amenable for CO_2 storage (Davidson, 2011). IGCC coal-based power plants offer several advantages such as: the potential gasification of multiple fuels/feedstocks (coal, petroleum coke, biomass) along with the production of various products (from electricity to hydrogen), efficiency gains when compared to conventional coal-based power plants and the need for smaller removal systems because of the relatively smaller volumes of syngas (being discharged at high pressure) compared to flue gas from existing power plants (Fernando, 2008; Haszeldine, 2009). Additionally, the higher concentrations (>40%) of CO_2 in the shifted syngas stream allows for bulk removal commercial methods to be used, such as absorption in chilled methanol or ethylene glycol, i.e., the Selexol™ or Rectisol® processes, respectively (Chalmers, 2010; Fernando, 2008). Nevertheless, these processes are energy intensive due to their heat transfer requirements so they are likely to be replaced if higher performance and less costly technologies are demonstrated (Figueroa et al., 2008).

Advanced pre-combustion capture technologies have been explored recently aiming to achieve a higher level of CO_2 capture than the conventional technologies at lower capital and operating costs (Hufton et al., 2011; Klara and Plunkett, 2010; Kunze and Spliethoff, 2012; Merkel et al., 2012). Novel approaches include adsorption with solid sorbents (Schell et al., 2009; Wang et al., 2011; Xiao et al., 2009), which may provide cost benefits over state-of-the-art physical solvent-based processes. Although no commercially available adsorption process for pre-combustion capture still exists, scientific research on the field has significantly increased over the last years (Blomen et al., 2009; Quintella et al., 2011), so the adsorption technology has become a promising one to reduce capture costs in a mid- to long-term scenario.

Solid adsorbents are employed in unsteady and cyclic processes composed of adsorption and regeneration steps. A high CO_2 selectivity and adsorption capacity are key properties of an adsorbent material for the separation of CO_2 from pre-combustion gas, i.e., CO_2/H_2 gas mixtures. However, of equal importance are the ease of regeneration and the lifetime of the adsorbents. Regeneration or reactivation of the adsorbent aims to restore the adsorption capacity of the exhausted adsorbent for its recyclic use as well as to recover valuable components present in the adsorbed phase, if any. Since adsorption operations are cyclic, the efficiency and cost of regeneration play important roles in the

overall feasibility of the process (Suzuki, 1990). Several alternative processes are available for the regeneration of spent adsorbents: 1) desorption by reducing the total pressure of the system (pressure swing adsorption, PSA), 2) desorption by raising the temperature (temperature swing adsorption, TSA), since the adsorption isotherm at higher temperatures is considerably advantageous for desorption, or 3) the combination of desorption at low pressure and high temperature, which is the principle of the pressure and temperature swing adsorption (PTSA) operation. When the component of interest has a high concentration in the feed stream (e.g., 10 percent or more), a PSA mechanism is more appropriate than a TSA one (Ruthven, 1984).

Activated carbons (AC) are competitive materials for capturing CO_2 in IGCC processes due to their low cost, high surface area and amenability to pore structure modification and surface functionalization (Wang et al., 2011). Additionally, they show higher CO_2 adsorption capacities at high pressures than other materials such as zeolites, as well as lower values of the heat of CO_2 adsorption. This property makes AC especially promising for applications in which the energy requirement for adsorbent regeneration is a critical factor, since less energy would be required for desorption (Choi et al., 2009).

The design and efficiency of an adsorption process is controlled by the overall dynamics of the fixed-bed, and the regeneration or desorption step is often the cost-determining factor of the separation process. The closest application of an adsorption process for CO_2 separation is the pressure swing adsorption (PSA) process for H_2 purification from syngas, which is well-known due to the large scale of H_2 production in petrochemical industries (Ciferno et al., 2011). However, in that CO_2/H_2 separation the desired product (H_2) is essentially non-adsorbed and can be obtained at high purity (99.9999%). Therefore, new methods to modify the process in order to meet the requirements of pre-combustion CO_2 capture need to be developed and implemented.

Response surface methodology (RSM) is a multivariate statistical technique used to optimize processes, i.e., to elucidate the conditions at which to apply a procedure in order to obtain the best possible response in the experimental region studied. This methodology involves the design of experiments and multiple regression analysis as tools to assess the effects of two or more independent variables on dependent variables (Myers and Montgomery, 1995). One additional advantage is the possibility of

evaluating the interaction effect between the independent variables on the response. This technique is based on the fit of a polynomial equation to the experimental data, to describe the behaviour of a given set of data. Thus, mathematical equations which describe the studied process are generated. The objective of this technique is to simultaneously optimize the levels of the studied variables in order to attain the best process performance (Bezerra et al., 2008). Recently, a few studies have been published on the application of RSM in matters related to CO_2 adsorption, reflecting the possibilities of this methodology. Thus, García et al. (García et al., 2011) studied the CO_2 equilibrium adsorption capacity and breakthrough time in a flow-through system where a commercial activated carbon was subjected to consecutive adsorption-desorption cycles. Serna-Guerrero et al. (Serna-Guerrero et al., 2010) studied the optimum regeneration conditions (temperature, pressure and flow rate of purge gas) of an amine-bearing adsorbent for CO_2 removal at low concentration (5%) and ambient temperature in a magnetic suspension balance, while Mulgundmath and Tezel (Mulgundmath and Tezel, 2010) compared a PSA with a PTSA process for CO_2 recovery from a flue gas composition of 10% CO_2 in N_2 using zeolite 13X in an adsorption column. Regeneration conditions used in the PTSA cycle proved to be better for regaining maximum adsorption capacity than conditions used in the PSA cycle.

However, an statistical study on how the regeneration conditions affect the dynamic performance of a solid sorbent for pre-combustion CO_2 capture has, to the best of the authors knowledge, yet to be published. Thus, in the present work, the cyclic performance of a commercial activated carbon in a pre-combustion capture process, i.e., high CO_2 concentration and high pressure, as a function of different regeneration conditions has been evaluated by means of response surface methodology. A bench-scale adsorption unit is employed for generating the experimental data in a simulated pressure and temperature swing adsorption process. The objectives of this study were: (i) to assess the combined effects of desorption temperature (T_{des}), desorption pressure (P_{des}) and purge to feed ratio (P/F ratio) on: 1) CO_2 working capacity (q_{CO2}) or actual CO_2 uptake in a full cycle (difference between the amount of the heavy component adsorbed at the adsorption pressure and the amount that remains adsorbed at the desorption/evacuation pressure); 2) yield or CO_2 recovery, which is the percentage of the total mass of CO_2 adsorbed in the adsorption step that is recovered in the desorption

step; 3) cycle throughput or productivity, which is defined as the working capacity divided by cycle time; 4) maximum rate of desorption ($r_{max\ des}$), i.e., how fast the material is regenerated and 5) raffinate (less strongly adsorbed component, i.e., H_2) and extract (more strongly adsorbed component, i.e., CO_2) purities, which are calculated as the measured time-averaged concentrations of H_2 and CO_2 at the outlet of the system in the adsorption and desorption steps, respectively; (ii) to determine the optimum values of the operating variables that maximize the response variables within the experimental region under study.

2. Materials and methods

2.1. Materials

A commercial steam activated peat-based extruded carbon supplied by Norit (Norit R2030CO2) was chosen as the adsorbent material for this study. A fully detailed chemical and textural characterization of this carbon, as well as its physical properties, has been reported previously (García et al., 2011; Pevida et al., 2008).

2.2. Cyclic adsorption-desorption experiments in a fixed-bed reactor

A single-bed adsorption unit packed with approximately 3 g of adsorbent (length: 11.1 cm, diameter: 0.9 cm, porosity: 0.49) has been used to conduct the cyclic adsorption-desorption experiments. The schematic and detailed description of the fixed-bed reactor can be found elsewhere (García et al., 2011).

For the experiments in this study a $CO_2/H_2/N_2$ gas mixture was used as the influent gas stream in the adsorption step, and N_2 was used as the inert carrier in the desorption step. Firstly, the adsorbent is dried (i.e., cleaned) by flowing N_2 (50 mL min^{-1} STP) for 50 min at 100°C and atmospheric pressure. After the drying step, the bed temperature and pressure are raised to the adsorption values in a pre-conditioning step of 10 min, where 60 mL min^{-1} (STP) of N_2 are allowed to flow through the system. This is followed by the adsorption step in which a $CO_2/H_2/N_2$ gas mixture (20/70/10% v/v) is fed through the pre-cleaned and pre-conditioned column (filled with N_2 at the adsorption temperature and pressure) for 10 min. The adsorption process was carried out at 15 bar of pressure and 25°C of temperature as these conditions gave the maximum values of breakthrough time and CO_2 equilibrium capture capacity in previous studies conducted

in our research group (García et al., 2011). A total flowrate of 100 mL min^{-1} (STP) was kept constant during the adsorption step. This step was terminated before the CO_2 broke through the bed, i.e., bed saturation was not reached, and CO_2 composition in the column effluent gas stream was continuously monitored as a function of time. The regeneration step followed and it was ended before the bed was fully desorbed. CO_2 desorption was accomplished by a pressure and temperature swing process where the pressure was reduced and temperature was raised. The bed temperature was controlled by coupling a heating element coiled around the reactor to an air-cooling device. As for the bed pressure, it was controlled by means of a back-pressure regulator located in the outlet pipe. A purge gas (N_2) was also used for recovering the CO_2 previously retained in the adsorption step. The purge to feed (P/F) ratio was defined as the relationship between the flow rates of purge and feed, measured at STP conditions. Different temperatures, pressures and purge/feed ratios were used in the desorption step. Desorption temperature varied from 60 to 140 ºC, desorption pressure between 1 and 5 bar and P/F ratio was studied between 0.05 and 1.00.

The duration of the desorption process was set to be the same as the adsorption one (10 min) to simulate operation with two beds, where the feed gas passes down through one of the beds while the other is being regenerated. Hence, the complete cycle time was set to be 20 minutes for the given CO_2 concentration (20%) in the feed. The composition of the outlet gas stream was measured with a dual channel micro-gas chromatograph (micro-GC), fitted with a thermal conductivity detector (TCD) in which He and Ar are used as the carrier gases.

The efficiency of the regeneration step, which will affect the amount of adsorbate remaining in the bed at the beginning of the next adsorption step, was dependent on the regeneration conditions used. For each experimental run the adsorbent was subjected to ten consecutive adsorption-desorption cycles. Measurement of the CO_2 elution profiles during the desorption step provided data on the effectiveness of adsorbate recovery, on working capacity, adsorbent throughput or productivity, rate of desorption and raffinate and extract purities.

2.3. Response Surface Methodology

Independent variables or factors are experimental variables that can be changed irrespectively of each other. In this work, they were the desorption temperature (T_{des}), desorption pressure (P_{des}) and purge to feed ratio (P/F ratio). The levels of these variables are the different values at which the experiments must be carried out. In this case, the three independent variables were investigated at five levels. T_{des} was studied between 60 and 140 ºC, P_{des} between 1 and 5 bar, whereas P/F ratio was studied between 0.05 and 1.00. The responses or dependent variables are those which are measured during the experiments. Herein, targeted response variables were the CO_2 working adsorption capacity (q_{CO2}), CO_2 recovery, adsorbent productivity, raffinate (H_2) purity, product (CO_2) purity and maximum rate of desorption ($r_{max\ des}$).

The experimental design used in this study was the central composite design (CCD), which defined the experiments needed to be carried out in the experimental region under consideration, i.e., the set of different combinations for the levels of the independent variables that were applied experimentally to obtain the responses. The CCD design was presented by Box and Wilson (Box and Wilson, 1951). This design consists of the following parts: (1) a full factorial design; (2) a star design in which experimental points are at a certain distance, α, from its centre and (3) a replicated central point. The α-value depends on the number of variables, k, and can be calculated by $\alpha=2^{k/4}$, so, for three variables, it is 1.682. The CCD is a better alternative to the full factorial three-level design since it demands a smaller number of experiments while providing comparable results (Ferreira et al., 2007). In the present study, the CCD design involved 20 experiments, including eight factorial points (2^3 full factorial design), six axial points and six replicates of the centre of the design. The experiments were conducted in a random order. To apply the RSM, the levels of the independent variables were coded in order to be able to compare variables with different units or of different orders of magnitude, so that they will all affect the response evenly, making the units of the parameters irrelevant. Codification of the levels of the variables consisted in transforming each real value into coordinates inside a scale with dimensionless values, which are proportional to their location in the experimental space. Table 1 shows the coded (in parentheses) and the decoded values of the independent

variables (T_{des}, P_{des} and P/F ratio), together with the experimental values for the response variables (q_{CO2}, CO_2 recovery, productivity, H_2 purity, CO_2 purity and $r_{max\ des}$). The mathematical-statistical treatment of experimental data consisted in fitting a polynomial function to the set of data collected from CCD. In this work, which employed three independent variables, x_1 (T_{des}), x_2 (P_{des}) and x_3 (P/F ratio), the following second-order polynomial equation was applied:

$$y = \beta_0 + \beta_1 x_1 + \beta_2 x_2 + \beta_3 x_3 + \beta_{11} x_1^2 + \beta_{22} x_2^2 + \beta_{33} x_3^2 + \beta_{12} x_1 x_2 + \beta_{13} x_1 x_3 + \beta_{23} x_2 x_3 + \beta_{123} x_1 x_2 x_3 + \varepsilon \quad (1)$$

where y is the response variable; β_0 is the constant term; β_1, β_2 and β_3 represent the coefficients of the linear parameters; β_{11}, β_{22} and β_{33} represent the coefficients of the quadratic parameters; β_{12}, β_{13}, β_{23} and β_{123} represent the coefficients of the interaction parameters and ε is the residual associated with the experiments. Multiple regression analysis was used to fit Eq. (1) to the experimental data by means of the method of least squares, which makes it possible to determine the β coefficients that generate the lowest possible residual. The equation obtained describes the behaviour of the response in the experimental region as a function of the independent variables. In order to evaluate the fitness of the quadratic model to the experimental data, tests for the significance of the regression model and the individual model coefficients were performed. This statistical evaluation of the models was performed by analysis of variance (ANOVA). The central idea of ANOVA is to compare the variation due to the treatment (change in the combination of variable levels) with the variation due to random errors inherent to the measurements of the generated responses (Vieira and Hoffman, 1989). From this comparison, it is possible to evaluate the significance of the regression used to foresee responses considering the sources of experimental variance. So, the ANOVA tests show which of the proposed models are statistically significant. The p-value is a parameter related to the comparison of the explained and residual variances of the data and it is used to establish whether a model or parameter is significant (p-value<0.05 at a confident level of 95%). The accuracy of the fitted polynomial model was expressed by the coefficient of determination R^2, which represents the proportion of variability in a set of data that is accounted for a statistical model. However, R^2 increases as the number

of variables in the model increases. It is therefore more appropriate to use Adj-R^2, which penalizes the statistic R^2 as extra variables are included in the model. In fact, Adj-R^2 decreases if unnecessary terms are added. The statistical analyses were carried out using SPSS Statistics 19.0 software.

To visualize the combined effects of two factors on any response, the model obtained can be three-dimensionally represented as a surface (response surface plot) and the best operation conditions inside the experimental region studied can be found by visual inspection. The two-dimensional display of the surface plot generates the contour plot, in which the lines of constant response are drawn on the plane of the two independent variables. Response surface and contour plots were generated using SigmaPlot 10.0 software. Then, the optimum values for each independent variable that would produce the best response in the experimental region under study were obtained.

3. Results and discussion

3.1. Evaluation of the cyclic adsorption-desorption performance by means of response surface methodology

The cyclic performance of the activated carbon was based on the analysis of the following parameters or response variables: CO_2 working capacity, CO_2 recovery, cycle productivity, maximum rate of desorption and raffinate (H_2) and product (CO_2) purities.

The experimental values obtained for the response variables are presented in Table 1. Tables 2 and 3 show the results of the fit of Eq. (1) to the experimental data by multiple regression analysis and those of the evaluation of the fitness of the model by ANOVA, together with the R^2 values.

The ANOVA tests showed which of the terms of the models were statistically significant to a 95% confidence level (p-value<0.05), and those that were not statistically significant (p-value>0.05) were eliminated from the models. It can also be observed that the models obtained were statistically significant to a 95% confidence level (p-value<0.05) for all the response variables studied. T_{des} and P/F ratio have a significant effect on q_{CO2}, CO_2 recovery, productivity (Table 2) and H_2 purity (Table 3), whereas P_{des} showed a non-significant influence on these response variables. However, the three independent variables studied have a significant influence on CO_2 purity and $r_{max\ des}$ (Table 3). On the other hand, no interaction effect between none of the three

independent variables was found, since the interaction terms in the models, x_1x_2, x_1x_3 and x_2x_3, proved to be statistically non-significant to a 95% confidence level (p-value>0.05). Once the non-significant terms were eliminated, the coded coefficient values were decoded in order to obtain the polynomial models for the response variables as a function of the actual independent variables. The obtained mathematical equations are shown in Table 4.

The regression equations for q_{CO2}, CO_2 recovery, productivity and H_2 purity show that these variables depend directly on T_{des} and P/F ratio and inversely on the square of P/F ratio, but they are not influenced by P_{des}. However, $r_{max\ des}$ depends directly on T_{des}, but inversely on P_{des} and P/F ratio. On the other hand, it can be observed that CO_2 purity depends inversely on T_{des} and P/F ratio, but directly on P_{des}.

Response surface and contour plots for q_{CO2}, CO_2 recovery, productivity and H_2 purity as a function of T_{des} and P/F ratio are presented in Fig. 1. Desorption pressure, $P_{des,}$ has not been included because it does not have a significant influence on these response variables. For q_{CO2} and productivity, the obtained graph had to be constraint by a plane surface due to the maximum boundary set by the conditions used in the experimental runs, i.e., maximum q_{CO2} is given by the CO_2 uptake in a full cycle when complete regeneration is achieved. Likewise, the maximum boundary for the adsorbent productivity would be given by the aforementioned working capacity divided by cycle time. Obviously, the highest possible value for CO_2 recovery and H_2 purity would be 100% so a plane surface was also included in Fig. 1 to account for this maximum limit. It can be observed that q_{CO2}, CO_2 recovery, productivity and H_2 purity increase as T_{des} increases. In addition, there is a curvature in the response surface and the contour plot isolines, which indicates that the effect of the P/F ratio on these response variables varies over the experimental range studied. Thus, at low desorption temperatures (<70°C), as P/F ratio increases from 0.05, a marked increase in the response variables is observed up to a maximum value, which is not the one given by boundary conditions, i.e., by plane surfaces. When T_{des} reaches 70°C and P/F ratio 0.93, the value on the plane surface for each response variable is attained, i.e., 2.8349 mol kg^{-1}, 100%, 8.5048 mol kg^{-1} h^{-1} and 100% for q_{CO2}, CO_2 recovery, productivity and H_2 purity, respectively. Higher P/F ratios would not increase the response any further. Likewise, for T_{des} higher than 70°C, there is a range of P/F ratios under which the responses increase as the P/F

ratio increases, up to a certain P/F ratio at which the response variable reaches its highest maximum value. Then, for a given T_{des} it is clear that the benefit of increasing the P/F ratio can only be achieved if the P/F ratio is lower than the aforementioned value. As an example, for a T_{des} of 90°C the P/F ratio that is needed for the response to reach its boundary limit is 0.62. The higher the T_{des} goes, the lower that P/F ratio needs to be in order to obtain the maximum possible response.

Fig. 1 also shows that the P/F ratio has a greater influence on the above response variables than T_{des}, since an increase in the P/F ratio value has a higher effect on the response than an increase in T_{des} within the experimental region studied.

These findings are not in agreement with previous studies under post-combustion conditions (Serna-Guerrero et al., 2010), that claimed the desorption temperature as the variable with the strongest impact on CO_2 working adsorption capacity at room temperature. However, in their case, the CO_2 was strongly bound to the amine-functionalized adsorbent by chemical adsorption as opposed to our case where physical adsorption is responsible for the CO_2 affinity for the activated carbon surface. Also, a post-combustion study with zeolite 13X (Mulgundmath and Tezel, 2010) revealed that purge time had the most significant effect on CO_2 recovery under their range of experimental conditions (purge time between 1 and 1.5 h, P/F ratio from 0.75 to 1 and purge gas temperature from 80 to 105°C), followed by P/F ratio and purge temperature. In the study presented here, purge time has not been included as an independent variable so its effect on response variables cannot be assessed. Even though a different interaction adsorbate-adsorbent along with a different experimental range and conditions were reported in the work conducted by Mulgundmath and Tezel (Mulgundmath and Tezel, 2010), P/F ratio and purge temperature were also identified as the variables with significant effects in our study.

The stability of an adsorbent material under a given set of regeneration conditions is associated with the change in adsorption capacity between consecutive cycles. As an illustrative example, Fig. 2 shows values of q_{CO2} along ten consecutive adsorption-desorption cycles for some arbitrary experimental runs. The working adsorption capacity for the first cycle has not been included since it corresponds to a fresh bed, free of adsorbate after the drying step, as opposed to the rest of the cycles, where a small amount of CO_2 gas remained in the adsorbent bed depending on the efficiency of the

regeneration step. Although not presented here, all the experiments showed very good cyclability, where the net CO_2 uptake in recurring adsorption/desorption cycles did not change significantly. Hence, under all the regeneration conditions studied the activated carbon showed an excellent reversibility, which has been attributed previously to the moderate adsorption strength or surface affinity of these materials for CO_2 (Choi et al., 2009; Siriwardane et al., 2001).

Fig. 3 shows the response surface and contour plots for the maximum rate of desorption as a function of T_{des} and P_{des} (Fig. 3a) and as a function of T_{des} and P/F ratio (Fig. 3b). It can be observed that $r_{max\ des}$ increases with the increase of T_{des} and the decrease of P_{des} and P/F ratio. The coefficient values of the polynomial models presented in Table 3 are coded coefficients since the values of the independent variables from which they were derived were also coded. Coded coefficients allow comparing the relative influence of the factors on the response variable. In the case of $r_{max\ des}$, Table 3 shows that the coded coefficient is higher for T_{des} than for P_{des} and P/F ratio. This fact indicates that a temperature swing is more efficient for fast CO_2 desorption than a pressure swing or a lower P/F ratio. In previous studies, it has already been found that heating was very efficient for desorbing carbon dioxide (Merel et al., 2008; Mulgundmath and Tezel, 2010; Plaza et al., 2010; Serna-Guerrero et al., 2010; Tlili et al., 2009). Within the experimental region under consideration, the maximum value of $r_{max\ des}$ (54.16 %v/v min^{-1}) was obtained at 140 ºC, 1 bar and a P/F ratio of 0.05.

Fig. 4 shows the response surface and contour plots for the CO_2 purity as a function of P_{des} and P/F ratio (Fig. 4a) and as a function of T_{des} and P/F ratio (Fig. 4b). It is clear from these plots that under the conditions used in this study, as P_{des} increases so does the CO_2 purity, as opposed to an increase in T_{des} and P/F ratio that lowers the purity of the CO_2 stream. Hence, T_{des} and P_{des} have an opposite effect on CO_2 purity than on $r_{max\ des}$, which is associated with the CO_2 purity being calculated as a time-averaged concentration. Thus, a higher T_{des} renders a faster CO_2 desorption process so a large portion of the adsorbed carbon dioxide can be recovered shortly after the desorption step begins. At the same time, the remaining gas stream components are also exiting the bed, resulting in a lower time-averaged CO_2 concentration than in those cases where the CO_2 is desorbed slower, i.e., at decreasing T_{des}, but in a more sustained way. Pressure ratio (adsorption/desorption) also plays a critical role in the concentration or purity of

the CO_2 obtained in the enriched product, that is, a decrease of the pressure ratio by increasing the desorption pressure improves the purity. Furthermore, the coded coefficients obtained for the CO_2 purity (Table 3) indicate that the P/F ratio is the most influential variable on CO_2 purity, followed by T_{des} and P_{des}. Within the experimental region under consideration, the maximum value of CO_2 purity (91.59 %) was obtained at 60 ºC, 5 bar and a P/F ratio of 0.05.

3.2. Discussion and implication for the separation of CO_2 from pre-combustion gas

The performance of a separation process is commonly measured by three parameters: (1) product purity, (2) product recovery and (3) adsorbent productivity. For a given separation, the product purity is predetermined, the energy requirement is usually proportional to the recovery, and the size of the adsorbent bed is inversely proportional to the adsorbent productivity. It is important to bear in mind that these three parameters are interrelated for any given PSA process (Yang, 2003).

Adsorption working capacity, which is the CO_2 loading difference between the spent and regenerated sorbent, will influence the required sorbent inventory of the process and hence equipment size. Although differences were observed under different regeneration conditions, a working capacity close to the maximum (2.8349 mol kg^{-1}) was achieved in the experimental runs (ranging from 95% to 100% of that maximum capacity), which is indicative of an effective regeneration process and fast adsorption kinetics in the fixed bed column. The higher the working capacity of an adsorbent for CO_2, the greater is the CO_2 recovery rate per unit weight of adsorbent, i.e., adsorbent productivity, as it was demonstrated in all the experiments conducted herein. Maximum values of CO_2 working capacity and productivity are desired since by increasing them, a smaller adsorber volume would be required. Therefore, the capital and operating costs would decrease. In order to increase the operating capacity, the residual carbon dioxide could be further eluted by an inert purge, which partially cools the bed for the subsequent adsorption step, but it would also dilute the CO_2 stream. Additionally, costs could be further reduced if increases in adsorbent working capacity and productivity are coupled with increases in the CO_2/H_2 selectivity. Hence, maximum q_{CO2} and productivity values presented here could be increased if the CO_2-adsorbent interaction is enhanced by, for instance, increasing the adsorbent alkalinity via surface modification. Impregnation with

additives and incorporation of basic nitrogen groups into the carbon framework are some approaches that have been investigated (Arstad et al., 2008; Kim et al., 2005; Pevida et al., 2008; Plaza et al., 2007; Plaza et al., 2008).

The CO_2 recovery obtained in the experiments conducted here ranged from 95.58 to 100% but in a CO_2 capture and sequestration scenario a high product yield is not as important as CO_2 purity. In a real capture operation, if recovery rates are low (< 90%), they can be increased by including additional steps in the cycle and by increasing the number of adsorbent beds, but these modifications increase the capital cost.

Under the conditions used in this study, the purge to feed ratio and desorption temperature were found to be key parameters that affect adsorbent working capacity, product recovery, adsorbent productivity and H_2 purity. Increasing the pressure ratio by decreasing the pressure in the desorption step did not improve any of the above variables. For PSA processes operating under vacuum desorption conditions, the pressure ratio was shown to play a critical role in the CO_2 recovery and the purity of the weakly adsorbed product (Ho et al., 2008). When the evacuation pressure was lower, there was a large driving force for the liberation of CO_2, and more CO_2 was recovered from the adsorbed bed. However, under the range of desorption conditions studied here, the pressure ratio did not play a significant role and CO_2 could be desorbed at relatively high pressure with a consequent saving on compression costs. If complete adsorbate removal is needed, the bed can be completely regenerated by using desorption temperatures as low as 70°C and purge to feed ratios of 0.93. An alternative is to increase the desorption temperature so a lower P/F ratio can be used to displace the CO_2 from the adsorbent bed.

H_2 purity was above 98% in all the studied cases. The hydrogen derived from the separation process can be used for power generation, i.e., can be burnt in the syngas turbine, or for some other purpose. Depending on the end-use of the produced hydrogen, its purity will vary; for instance, in fuel cell applications, hydrogen with a purity of over 99.99% is required, otherwise their lifetime decreases rapidly (Lopes et al., 2011). Thus, for some processes, an additional H_2 purification process would be required in order to meet the end-use specifications.

The stability of the material during extensive adsorption-desorption cycling determines the lifetime of the adsorbent and is of importance in determining the rate of adsorbent

replacement. Hence, it is a key property of equal importance as the CO_2 adsorption capacity because of its direct impact on the economics of any commercial scale operation. The activated carbon presented here proved to be very stable under all the regeneration conditions studied, in accordance with previous works that had already claimed the ease of regeneration and excellent reversibility presented by activated carbons when compared with other materials such as zeolites (Choi et al., 2009).

Of the most importance to a CO_2 capture process with respect to the subsequent CO_2 transport and storage, is the purity of the CO_2 product stream. A large nitrogen to feed ratio leads to the desorption of the adsorbate diluted in the purge gas, i.e., the CO_2 purity in the product stream is reduced. Likewise, the maximum rate of CO_2 desorption is favoured at low purge to feed ratios. Hence, low P/F ratio values are desirable when aiming at pure CO_2 streams. The adsorbate will be displaced by N_2, which is moderately adsorbed, and can be easily separated from the product. The purge effluent must be then treated in another smaller column to recover pure carbon dioxide. As expected, the highest product purity (91.59%) obtained in this work does not correspond to the best/optimum values of other parameters such as product recovery and adsorbent productivity. Combining heating and a large purge to feed ratio proved to be very efficient for eluting carbon dioxide from the bed, but it also resulted in the CO_2 purity being penalised. Thus, the optimal choice of desorption temperature and purge to feed ratio affects the process performance seriously. A relevant finding was that desorption pressure did not have a significant effect on product recovery and adsorbent productivity, whilst increasing desorption pressures favoured higher CO_2 purity streams under the studied experimental conditions. Therefore, higher desorption pressures could be used and the benefits would be then two-fold: not only the enriched product stream purity would be favoured, but also power requirements to compress and transport CO_2 will be much lower than if the CO_2 stream was at atmospheric pressure. Ultimately, economic analyses will be needed to determine which combination of properties will result in the lowest costs for a particular plant.

4. Conclusions

Response surface methodology was used to evaluate the performance of a commercial activated carbon in a PTSA process operated at simulated industrial shifted-syngas conditions and under different batchwise regeneration conditions. The combined effect of desorption temperature, desorption pressure and purge to feed ratio on CO_2 working adsorption capacity, CO_2 recovery, adsorbent productivity, raffinate (H_2) and extract (CO_2) purities and maximum rate of desorption was investigated.

No interaction effects between the independent variables on the responses were detected. The most influential variable on working adsorption capacity, CO_2 recovery, adsorbent productivity and raffinate purity was the P/F ratio. For T_{des} lower than 70°C, a P/F ratio increase led to a marked increase in the response variables, up to reach a maximum value. For a T_{des} of 70°C and a P/F ratio of 0.93 the highest maximum value for each response was attained; the more extra heating (above 70°C) was supplied, the less purge, i.e. P/F ratio, was needed to obtain the maximum possible response. A significant finding was that desorption pressure did not have a significant influence on the above variables in the considered experimental region.

As for the maximum rate of desorption, desorption temperature became the dominant factor; as T_{des} increased, a faster CO_2 desorption was observed, whereas an increase in desorption pressure and P/F ratio led to a decrease in this variable. The maximum value for the maximum rate of desorption within the experimental region studied was obtained at 140 ºC, 1 bar and a P/F ratio of 0.05. Finally, the P/F ratio had the strongest impact on the CO_2 purity, which depended inversely on desorption temperature and P/F ratio, but directly on desorption pressure. A maximum CO_2 purity of 91.59% was obtained at 60 ºC, 5 bar and a P/F ratio of 0.05.

With the aid of a statistical analysis technique, a preliminary screening on regeneration conditions using batch experiments has been conducted. The findings of this study provide a better understanding of the influence of different regeneration conditions and their interactions on the dynamic performance of an activated carbon in a fixed-bed pressure and temperature swing process. More importantly, and although an in-depth economical evaluation would be needed, the strategy followed in this work can be employed in the design of a proper regeneration process to be applied in a scaled-up PTSA system for pre-combustion CO_2 capture.

Acknowledgements

This work was carried out with financial support from the Spanish MINECO (Project ENE2011-23467), co-financed by the European Social Fund. M.V.Gil acknowledges funding from the CSIC JAE-Doc program, co-financed by the European Social Fund.

References

Arstad, B., Fjellvåg, H., Kongshaug, K., Swang, O., Blom, R., 2008. Amine functionalised metal organic frameworks (MOFs) as adsorbents for carbon dioxide. Adsorption 14, 755-762.

Bezerra, M.A., Santelli, R.E., Oliveira, E.P., Villar, L.S., Escaleira, L.A., 2008. Response surface methodology (RSM) as a tool for optimization in analytical chemistry. Talanta 76, 965-977.

Blomen, E., Hendriks, C., Neele, F., 2009. Capture technologies: Improvements and promising developments. Energy Procedia 1, 1505-1512.

Box, G.E.P., Wilson, K.B., 1951. On the experimental attainment of optimum conditions. J. R. Stat. Soc. B 13, 1-45.

Ciferno, J., Litynski, J., Brickett, L., Murphy, J., Munson, R., Zaremsky, C., Marano, J., Strock, J., 2011. DOE/NETL advanced carbon dioxide capture R&D program: technology update. National Energy Technolology Laboratory, USA, p. 516 pages.

Chalmers, H., 2010. Flexible operation of coal-fired power plant with CO_2 capture. IEA - Clean Coal Centre, p. 49.

Choi, S., Drese, J.H., Jones, C.W., 2009. Adsorbent materials for carbon dioxide capture from large anthropogenic point sources. ChemSusChem 2, 796-854.

Davidson, R.M., 2011. Pre-combustion capture of CO_2 in IGCC plants. IEA Clean Coal Centre, p. 98.

Fernando, R., 2008. Coal gasification. IEA Clean Coal Centre, p. 56.

Ferreira, S.L.C., Bruns, R.E., Paranhos da Silva, E.G., Lopes dos Santos, W.N., Quintella, C.M., David, J.M., Bittencourt de Andrade, J., Breitkreitz, M.C., Sales Fontes Jardim, I.C., Barros Neto, B., 2007. Statistical designs and response surface techniques for the optimization of chromatographic systems. Journal of Chromatography A 1158, 2-14.

Figueroa, J.D., Fout, T., Plasynski, S., McIlvried, H., Srivastava, R.D., 2008. Advances in CO_2 capture technology-The U.S. Department of Energy's Carbon Sequestration Program. International Journal of Greenhouse Gas Control 2, 9-20.

García, S., Gil, M.V., Martín, C.F., Pis, J.J., Rubiera, F., Pevida, C., 2011. Breakthrough adsorption study of a commercial activated carbon for pre-combustion CO_2 capture. Chemical Engineering Journal 171, 549-556.

Haszeldine, R.S., 2009. Carbon Capture and Storage: How Green Can Black Be? Science 325, 1647-1652.

Ho, M.T., Allinson, G.W., Wiley, D.E., 2008. Reducing the cost of CO_2 capture from flue gases using pressure swing adsorption. Industrial & Engineering Chemistry Research 47, 4883-4890.

Hufton, J., Golden, T., Quinn, R., Kloosterman, J., Wright, A., Schaffer, C., Hendershot, R., White, V., Fogash, K., 2011. Advanced hydrogen and CO_2 capture technology for sour syngas. Energy Procedia 4, 1082-1089.

Kim, S., Ida, S., Guliants, V.V., Lin, J.Y.S., 2005. Tailoring pore properties of MCM-48 silica for selective adsorption of CO_2. Journal of Physical Chemistry B. 109, 6287-6293.

Klara, J.M., Plunkett, J.E., 2010. The potential of advanced technologies to reduce carbon capture costs in future IGCC power plants. International Journal of Greenhouse Gas Control 4, 112-118.

Kunze, C., Spliethoff, H., 2012. Assessment of oxy-fuel, pre- and post-combustion-based carbon capture for future IGCC plants. Applied Energy 94, 109-116.

Lopes, F.V.S., Grande, C.A., Rodrigues, A.E., 2011. Activated carbon for hydrogen purification by pressure swing adsorption: Multicomponent breakthrough curves and PSA performance. Chemical Engineering Science 66, 303-317.

Merel, J., Clausse, M., Meunier, F., 2008. Experimental investigation on CO_2 post-combustion capture by indirect thermal swing adsorption using 13X and 5A zeolites. Ind. Eng. Chem. Res. 47, 209-215.

Merkel, T.C., Zhou, M., Baker, R.W., 2012. Carbon dioxide capture with membranes at an IGCC power plant. Journal of Membrane Science 389, 441-450.

Mulgundmath, V., Tezel, F., 2010. Optimisation of carbon dioxide recovery from flue gas in a TPSA system. Adsorption 16, 587-598.

Myers, R.H., Montgomery, D.H., 1995. Response Surface Methodology. John Wiley & Sons, USA.

Pevida, C., Plaza, M.G., Arias, B., Fermoso, J., Rubiera, F., Pis, J.J., 2008. Surface modification of activated carbons for CO_2 capture. Applied Surface Science 254, 7165-7172.

Plaza, M.G., García, S., Rubiera, F., Pis, J.J., Pevida, C., 2010. Post-combustion CO_2 capture with a commercial activated carbon: comparison of different regeneration strategies. Chemical Engineering Journal 163, 41-47.

Plaza, M.G., Pevida, C., Arenillas, A., Rubiera, F., Pis, J.J., 2007. CO_2 capture by adsorption with nitrogen enriched carbons. Fuel 86, 2204-2212.

Plaza, M.G., Pevida, C., Arias, B., Fermoso, J., Arenillas, A., Rubiera, F., Pis, J.J., 2008. Application of thermogravimetric analysis to the evaluation of aminated solid sorbents for CO_2 capture. Journal of Thermal Analysis and Calorimetry 92, 601-606.

Quintella, C.M., Hatimondi, S.A., Musse, A.P.S., Miyazaki, S.F., Cerqueira, G.S., Moreira, A.d.A., 2011. CO_2 capture technologies: An overview with technology assessment based on patents and articles. Energy Procedia 4, 2050-2057.

Ruthven, D.M., 1984. Principles of adsorption and adsorption processes. John Wiley & Sons, New York.

Schell, J., Casas, N., Mazzotti, M., 2009. Pre-combustion CO_2 capture for IGCC plants by an adsorption process. Energy Procedia 1, 655-660.

Serna-Guerrero, R., Belmabkhout, Y., Sayari, A., 2010. Influence of regeneration conditions on the cyclic performance of amine-grafted mesoporous silica for CO_2 capture: An experimental and statistical study. Chemical Engineering Science 65, 4166-4172.

Siriwardane, R.V., Shen, M.-S., Fisher, E.P., Poston, J.A., 2001. Adsorption of CO_2 on molecular sieves and activated carbon. Energy & Fuels 15, 279-284.

Suzuki, M., 1990. Adsorption Engineering. Elsevier, Tokyo, Japan.
Tlili, N., Grévillot, G., Vallières, C., 2009. Carbon dioxide capture and recovery by means of TSA and/or VSA. International Journal of Greenhouse Gas Control 3, 519-527.
Vieira, S., Hoffman, R., 1989. Estatística Experimental, São Paulo.
Wang, Q., Luo, J., Zhong, Z., Borgna, A., 2011. CO_2 capture by solid adsorbents and their applications: current status and new trends. Energy & Environmental Science 4, 42-55.
Xiao, P., Wilson, S., Xiao, G., Singh, R., Webley, P., 2009. Novel adsorption processes for carbon dioxide capture within an IGCC process. Energy Procedia 1, 631-638.
Yang, R.T., 2003. Adsorbents: fundamentals and applications. John Wiley & Sons Inc., Hoboken, New Yersey.

Figure captions

Fig. 1. Response surface and contour plots as a function of desorption temperature, T_{des}, and purge to feed ratio, P/F ratio, for: (a) working adsorption capacity, q_{CO2}; (b) CO_2 recovery; (c) productivity; and (d) H_2 purity.

Fig. 2. Working adsorption capacity of activated carbon Norit R2030CO2 over various adsorption-desorption cycles run at different experimental conditions (see Table 1).

Fig. 3. Response surface and contour plots for maximum rate of desorption, $r_{max\ des}$, as a function of: (a) desorption temperature, T_{des}, and desorption pressure, P_{des}; and (b) desorption temperature, T_{des}, and purge to feed ratio, P/F ratio.

Fig. 4. Response surface and contour plots for product (CO_2) purity as a function of: (a); desorption pressure, P_{des}, and purge to feed ratio, P/F ratio, and (b) desorption temperature, T_{des}, and purge to feed ratio, P/F ratio.

Table 1. Independent variables and experimental values of the response variables for the central composite design (CCD)

Run	Independent variables			Response variables					
	T_{des} (ºC)	P_{des} (bar)	P/F ratio	q_{CO2} (mol kg^{-1})	CO_2 recovery (%)	Productivity (mol kg^{-1} h^{-1})	H_2 purity (%)	CO_2 purity (%)	$r_{max\ des}$ (%v/v min^{-1})
1	76 (-1)	1.8 (-1)	0.24 (-1)	2.8166	99.35	8.4498	99.72	82.81	35.00
2	124 (+1)	1.8 (-1)	0.24 (-1)	2.8330	99.93	8.4991	99.97	78.51	41.10
3	76 (-1)	4.2 (+1)	0.24 (-1)	2.7421	96.72	8.2262	98.65	84.63	31.56
4	124 (+1)	4.2 (+1)	0.24 (-1)	2.8255	99.67	8.4764	99.86	82.88	43.64
5	76 (-1)	1.8 (-1)	0.81 (+1)	2.8334	99.94	8.5001	99.98	73.92	31.98
6	124 (+1)	1.8 (-1)	0.81 (+1)	2.8349	100.00	8.5048	100.00	69.85	34.26
7	76 (-1)	4.2 (+1)	0.81 (+1)	2.8274	99.73	8.4822	99.89	83.50	22.88
8	124 (+1)	4.2 (+1)	0.81 (+1)	2.8342	99.98	8.5027	99.99	74.12	30.80
9[a]	100 (0)	3.0 (0)	0.53 (0)	2.8320	99.90	8.4960	99.96	78.78	30.79
10	60 (-1.682)	3.0 (0)	0.53 (0)	2.7933	98.53	8.3798	99.39	81.15	22.90
11	140 (+1.682)	3.0 (0)	0.53 (0)	2.8349	100.00	8.5046	100.00	74.41	46.15
12	100 (0)	1.0 (-1.682)	0.53 (0)	2.8349	100.00	8.5048	100.00	77.18	50.31
13	100 (0)	5.0 (+1.682)	0.53 (0)	2.8263	99.70	8.4790	99.87	79.24	25.14
14	100 (0)	3.0 (0)	0.05 (-1.682)	2.7095	95.58	8.1285	98.13	86.65	37.19
15	100 (0)	3.0 (0)	1.00 (+1.682)	2.8340	99.97	8.5021	99.99	73.20	28.49

[a]Central point mean of six replicates

T_{des}: desorption temperature; P_{des}: desorption pressure; P/F ratio: purge to feed ratio; q_{CO2}: working adsorption capacity for CO_2; $r_{max\ des}$: maximum rate of desorption.

Table 2. Results of multiple regression analysis and ANOVA for the fit of the polynomial model to the working adsorption capacity (q_{CO2}), CO_2 recovery and productivity experimental data

	q_{CO2} (mol kg^{-1})				CO_2 recovery (%)				Productivity (mol kg^{-1} h^{-1})			
	Coded coefficient	Sum of squares	DF[a]	*p*-value	Coded coefficient	Sum of squares	DF[a]	*p*-value	Coded coefficient	Sum of squares	DF[a]	*p*-value
Intersection	2.831	48.194	1	0.000[b]	99.873	59964.240	1	0.000[b]	8.494	433.74	1	0.000[b]
x_1	0.020	0.005	1	0.005[b]	0.695	6.597	1	0.005[b]	0.059	0.048	1	0.005[b]
x_2	-0.008	0.001	1	0.195	-0.267	0.973	1	0.195	-0.023	0.007	1	0.195
x_3	0.034	0.016	1	0.000[b]	1.218	20.248	1	0.000[b]	0.104	0.147	1	0.000[b]
x_1^2	-0.002	0.000	1	0.685	-0.078	0.088	1	0.684	-0.007	0.001	1	0.685
x_2^2	0.004	0.000	1	0.507	0.129	0.239	1	0.505	0.011	0.002	1	0.506
x_3^2	-0.011	0.002	1	0.066[b]	-0.385	2.142	1	0.067[b]	-0.033	0.015	1	0.068[b]
x_1x_2	0.009	0.001	1	0.234	0.317	0.806	1	0.234	0.027	0.006	1	0.236
x_1x_3	-0.000	0.000	1	0.978	-0.005	0.000	1	0.984	0.000	0.000	1	0.986
x_2x_3	0.009	0.001	1	0.217	0.330	0.871	1	0.218	0.028	0.006	1	0.217
$x_1x_2x_3$	-0.008	0.000	1	0.301	-0.275	0.605	1	0.298	-0.023	0.004	1	0.302
Model		0.026	10	0.005[b]		32.693	10	0.005[b]		0.237	10	0.005[b]
Residual		0.004	9			4.463	9			0.032	9	
Total		0.030	19			37.155	19			0.269	19	
R^2	0.879				0.880				0.880			
Adj-R^2	0.746				0.746				0.746			

x_1: T_{des}; x_2: P_{des}; x_3: P/F ratio

[a] Degrees of freedom; [b] statistically significant

Table 3. Results of multiple regression analysis and ANOVA for the fit of the polynomial model to raffinate (H_2) purity, extract (CO_2) purity and maximum rate of desorption ($r_{max\ des}$) experimental data

	H_2 purity (%)				CO_2 purity (%)				$r_{max\ des}$ (% v/v min^{-1})			
	Coded coefficient	Sum of squares	DF[a]	*p*-value	Coded coefficient	Sum of squares	DF[a]	*p*-value	Coded coefficient	Sum of squares	DF[a]	*p*-value
Intersection	99.947	60053.192	1	0.000[b]	78.775	37305.807	1	0.000[b]	30.835	5715.730	1	0.000[b]
x_1	0.293	1.169	1	0.006[b]	-2.258	69.621	1	0.006[b]	4.941	333.456	1	0.004[b]
x_2	-0.110	0.167	1	0.206	1.721	40.450	1	0.024[b]	-4.085	227.935	1	0.011[b]
x_3	0.515	3.625	1	0.000[b]	-3.665	183.500	1	0.000[b]	-3.369	155.015	1	0.028[b]
x_1^2	-0.029	0.012	1	0.723	-0.322	1.498	1	0.613	1.028	15.244	1	0.433
x_2^2	0.056	0.045	1	0.496	-0.170	0.418	1	0.788	2.159	67.225	1	0.119
x_3^2	-0.163	0.384	1	0.068[b]	0.436	2.739	1	0.497	0.433	2.699	1	0.738
x_1x_2	0.129	0.133	1	0.255	-0.345	0.952	1	0.686	1.453	16.878	1	0.410
x_1x_3	0.006	0.000	1	0.954	-0.925	6.845	1	0.292	-0.998	7.960	1	0.568
x_2x_3	0.134	0.143	1	0.238	0.958	7.334	1	0.276	-1.458	16.994	1	0.409
$x_1x_2x_3$	-0.111	0.099	1	0.321	-0.982	7.722	1	0.265	-0.042	0.014	1	0.980
Model		5.801	10	0.005[b]		321.590	10	0.007[b]		835.425	10	0.031[b]
Residual		0.806	9			49.147	9			203.873	9	
Total		6.607	19			370.737	19			1039.298	19	
R^2	0.878				0.867				0.804			
Adj-R^2	0.742				0.720				0.586			

x_1: T_{des}; x_2: P_{des}; x_3: P/F ratio

[a] Degrees of freedom; [b] statistically significant

Table 4. Polynomial models for the response variables as a function of the operation variables (T_{des} is the desorption temperature in ºC; P_{des} is the desorption pressure in bar; and P/F ratio is the purge to feed ratio)

Response	2nd order polynomial equations	Maximum possible values[a]
q_{CO2} (mol kg^{-1})	2.6474 + 0.0008 T_{des} + 0.2684 P/F ratio – 0.1394 (P/F ratio)^2	2.8349
CO_2 recovery (%)	93.3768 + 0.0292 T_{des} + 9.4468 P/F ratio – 4.8908 (P/F ratio)^2	---
Productivity (mol kg^{-1} h^{-1})	7.9418 + 0.0025 T_{des} + 0.8038 P/F ratio – 0.4159 (P/F ratio)^2	8.5048
H_2 purity (%)	97.2066 + 0.0123 T_{des} + 4.0052 P/F ratio – 2.0771 (P/F ratio)^2	---
CO_2 purity (%)	90.7025 – 0.0949 T_{des} + 1.4473 P_{des} – 12.9794 P/F ratio	---
$r_{max\ des}$ (% v/v min^{-1})	29.0996 + 0.2078 T_{des} – 3.4356 P_{des} – 11.9295 P/F ratio	---

[a] The maximum possible values are boundaries set by the specific conditions used in the experimental runs.

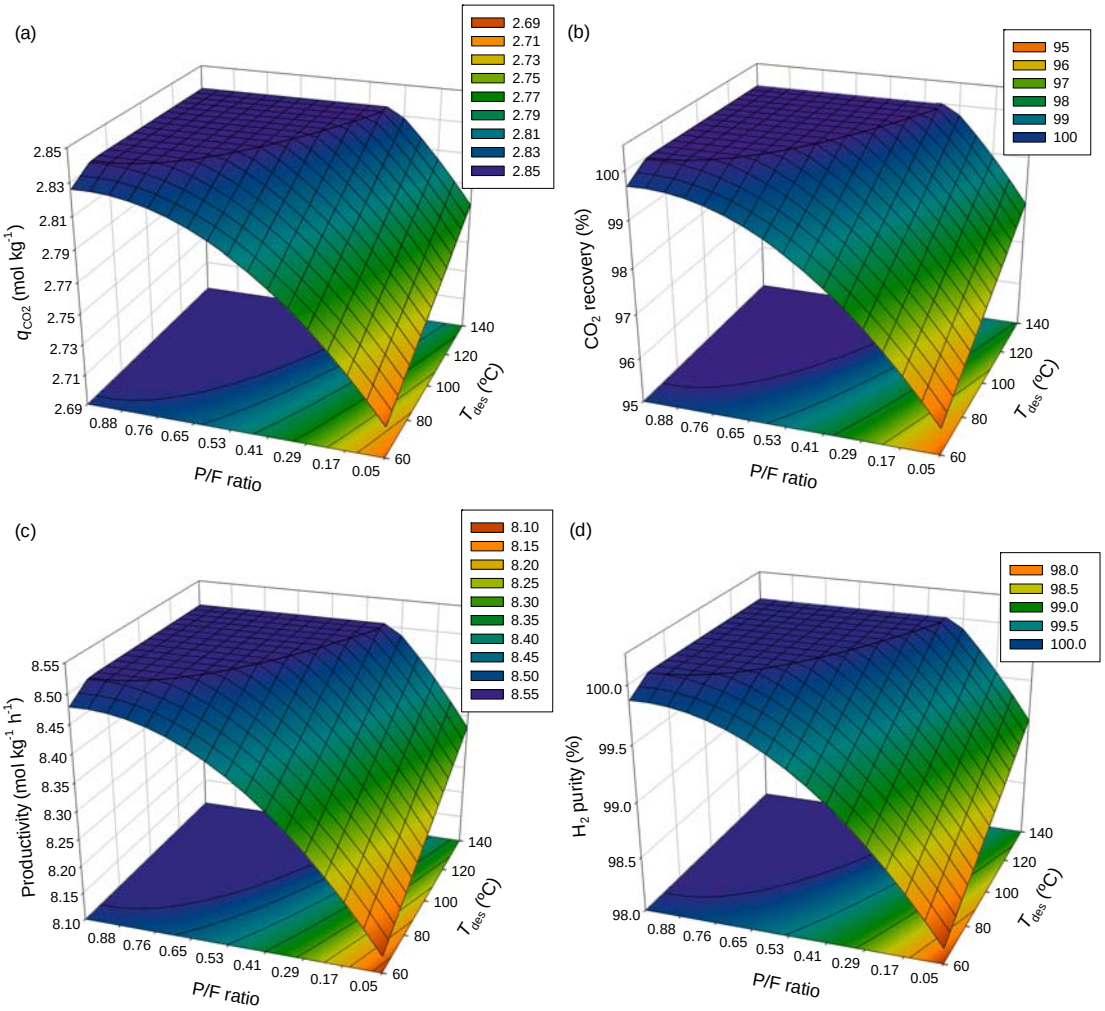

Fig. 1. Response surface and contour plots as a function of desorption temperature, T_{des}, and purge to feed ratio, P/F ratio, for: (a) working adsorption capacity, q_{CO2}; (b) CO_2 recovery; (c) productivity; and (d) H_2 purity.

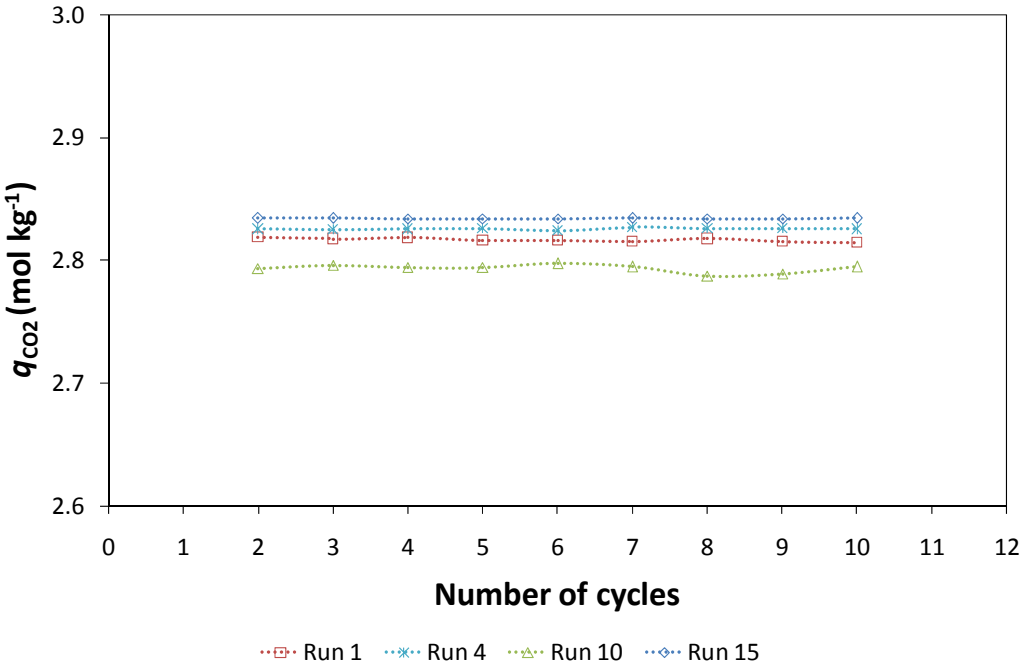

Fig. 2. Working adsorption capacity of activated carbon Norit R2030CO2 over various adsorption-desorption cycles run at different experimental conditions (see Table 1).

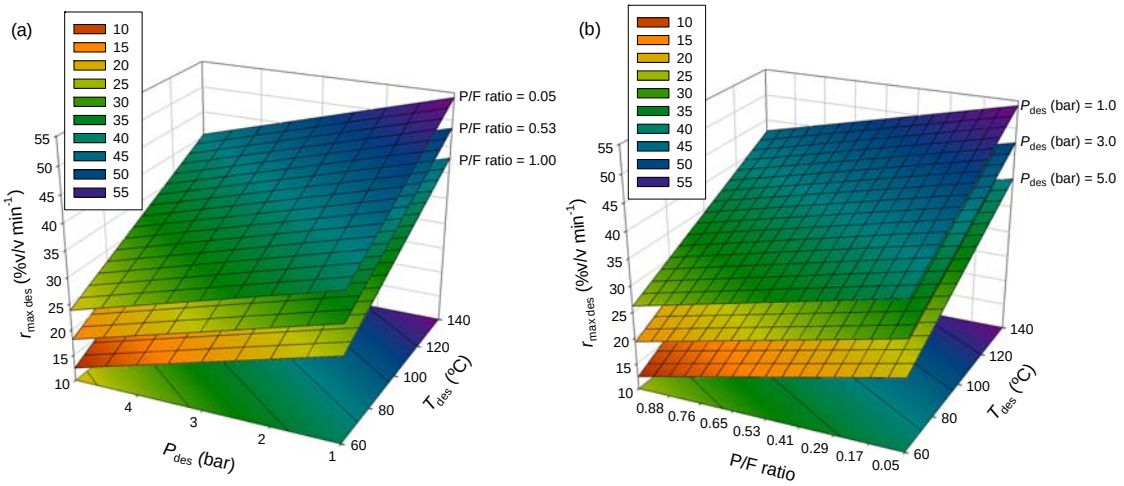

Fig. 3. Response surface and contour plots for maximum rate of desorption, $r_{\max\ \mathrm{des}}$, as a function of: (a) desorption temperature, T_{des}, and desorption pressure, P_{des}; and (b) desorption temperature, T_{des}, and purge to feed ratio, P/F ratio.

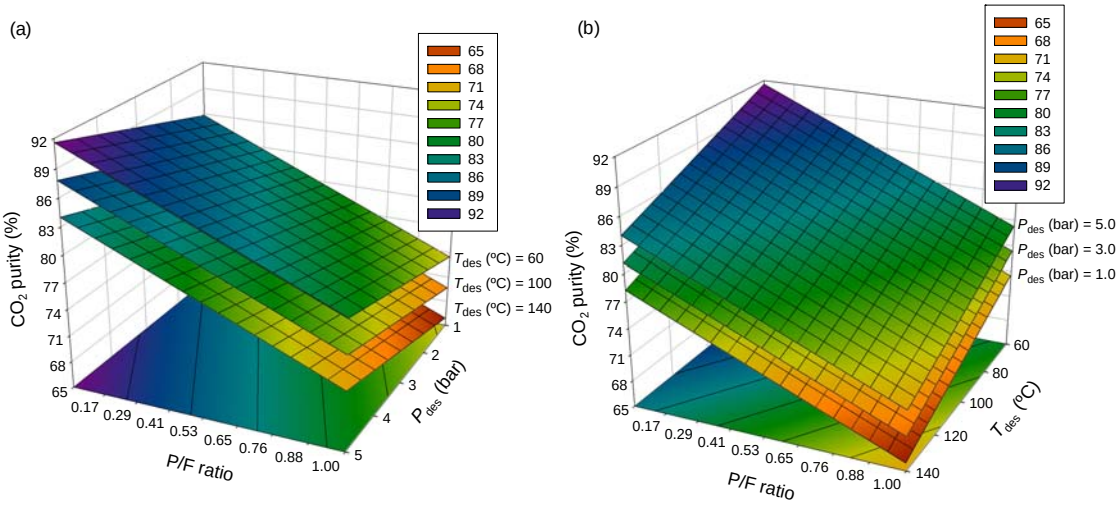

Fig. 4. Response surface and contour plots for product (CO_2) purity as a function of: (a); desorption pressure, P_{des}, and purge to feed ratio, P/F ratio, and (b) desorption temperature, T_{des}, and purge to feed ratio, P/F ratio.